JOURNAL OF AIRCRAFT
Vol. 38, No. 1, January–February 2001

Structural Loading of Outbound-Horizontal Stabilizer Aircraft Relative to Comparable Conventional Designs

J. A. C. Kentfield*
University of Calgary, Calgary, Alberta T2N 1N4, Canada

The objective was to study the aerodynamic and gravitational structural loadings, under steady, level, flight conditions, of aircraft with outboard horizontal-stabilizers (OHS). The aerodynamics of OHS configurations have been studied previously yielding results reported in the literature. The main reasons for interest in OHS configurations are explained briefly. The approach was based on evaluating by analytical means, structural loadings, predominantly, but not exclusively, consisting of wing-root bending moments and wing-root torsional loadings for OHS configurations. The corresponding, complementary, aerodynamic loadings were obtained from previously published data. The main conclusions from the work were that contrary to what might, at first glance, appear to be a problem OHS aircraft configurations do not suffer from excessive structural wing bending moments or torsional loadings relative to conventional designs of equal gross lift and main-plane (wing) aspect ratio nor do they appear to be more prone to flutter.

Nomenclature

A	=	aspect ratio
b	=	semispan
C_L	=	lift coefficient
C_m	=	pitching moment coefficient
c	=	average chord
F	=	aerodynamic force on horizontal stabilizer as a result of oscillation
H_v	=	height of vertical tails
K	=	elastic stiffness of tail structure
L	=	lift of aerodynamic surface
L'	=	distance from $c_w/4$ to $c_{TH}/4$
M	=	effective mass of tail
S	=	planform area
U	=	flight velocity
W	=	weight
x	=	distance aft from wing leading edge
θ	=	displacement (angular or linear) of oscillating tail from rest position

Subscripts

ac	=	aerodynamic center
(B + T)	=	boom plus tail
CONV	=	conventional configuration
cp	=	center of pressure
FL	=	fuel
MAX	=	maximum value
OHS	=	outboard horizontal stabilizer
TH	=	horizontal-tail surface
TV	=	vertical-tail surface
W	=	wing

Introduction

THE outboard-horizontal-stabilizer (OHS) concept places the horizontal stabilizer surfaces outboard, and downstream, of the main-plane tips of a monoplane in order to place the horizontal stabilizers in the upwash of the swirling flow generated by the lifting main plane. Each horizontal stabilizer is secured to a boom projecting downwind from the associated wing tip. Because each horizontal stabilizer lies in an upwash flow, it is, therefore, possible to use the horizontal stabilizers not only for pitch control, as in a conventional aircraft, but also as very efficient lifting surfaces because the lift-force vectors are, caused by the upwash flow in which each horizontal stabilizer is immersed, inclined forward in the flight direction, thereby helping to counter drag forces. In practice, in order to provide a pitch-control margin the horizontal stabilizer lift coefficient is arranged to be about half that of the mainplane during level flight.

Additionally the tail vertical surfaces, each attached to the upper surface of the downwind end of each tail-support boom, experience inflow as a result of the flowfield generated by the lifting wing, much in the manner of a winglet. The resulting inflow generates, on both vertical tail surfaces, a force acting inward toward the aircraft centerline and inclined in the flight direction. These forces also serve, therefore, to oppose drag.

Prior work served to verify both experimentally and also on an analytical basis the foregoing mode of operation of OHS configurations.[1–4] The main conclusions of this work were that typically an OHS configuration is about 15% smaller in wing planform area than an otherwise comparable conventional configuration of equal gross lift, at an equal mainplane lift coefficient, caused by the lift generated by the horizontal stabilizers of the OHS aircraft. Because of this factor and also the drag-opposing forces generated by the horizontal and vertical tail surfaces of an OHS vehicle, the drag of the OHS aerodynamic surfaces is, for a prescribed gross lift, typically about 30% less than that of a conventional configuration. Figure 1 shows, by way of an example, a sketch of an 18-passenger OHS-type, twin-engined commuter aircraft employing a centerline propulsion arrangement. Centerline propulsion is not an essential feature of the OHS concept and was selected merely for design simplicity.

The prime purpose of the study reported here was to investigate the structural feasibility, or otherwise, of the OHS concept by means of a preliminary design-type exercise targeted at establishing the critical structural loads acting on OHS commuter-style aircraft relative to those of comparable conventional vehicles. For the purposes of the study, critical structural loads were interpreted as bending and torsional loads acting at the main-plane roots. In addition, loads not active in conventional aircraft but deemed of importance for OHS designs were wing-tip torsion and bending and torsion in the tail support booms. The work also included a preliminary investigation of the propensity of OHS aircraft to suffer from flutter problems.

Background

In addition to the prior work, referred to earlier, undertaken at the University of Calgary,[1–4] students of the Department of Mechanical

Received 1 February 2000; revision received 16 August 2000; accepted for publication 17 August 2000.

*Professor, Department of Mechanical Engineering. Senior Member AIAA.

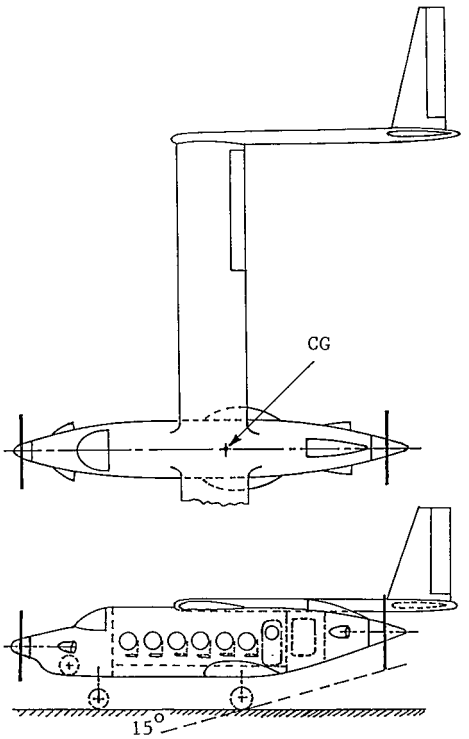

Fig. 1 OHS-type turboprop light transport. Approximately 18 passengers and centerline power plants.

and Manufacturing Engineering have built, and flown successfully, a number of large, approximately 3-m (10-ft) span, radio-controlled, powered, model OHS aircraft that have been entered in the annual Society of Automotive Engineers Aero Design contests. Here the objective is to lift the heaviest possible payload on the basis of an aircraft of prescribed maximum planform area and engine type. These models showed that OHS aircraft are stable, capable of controlled flight, and are competitive.

Perhaps the most relevant work prior to that carried out at the University of Calgary was undertaken in Germany during the Second World War by Blohm und Voss. This company designed a series of aft-swept-wing fighters, some powered with pusher piston engines, other by turbojets. These aircraft were, according to Internet information, designed by the Blohm und Voss chief designer Richard Vogt assisted by Hans Amtmann. Each design featured a short boom projecting downwind from each wing tip supporting a horizontal stabilizer projecting outboard of each wing tip. The leading edge of each stabilizer aligned with the wing trailing edge for most of the series. Also, in most cases, vertical stabilizer surfaces were omitted, reliance apparently being placed on a combination of wing dihedral in conjunction with horizontal stabilizer anhedral.

Further details of other projects that can be regarded as related to the OHS concept can be found elsewhere.[4]

Component Weight Distribution

The component weight distribution for use in the preliminary design exercise was selected on the basis of the published specifications of a number of relatively high-speed, conventional, turboprop-type commuter aircraft. These data, averaged and approximated appropriately, are presented in Table 1. Because the wing sections used in these commuter aircraft were not known, the decision was made to employ, for the study, wing airfoils having the characteristics of the NACA 2412 section and for the stabilizer surfaces NACA 0012. These choices are consistent with those of a previous study of the comparative aerodynamic performances of OHS and comparable conventional aircraft.[4] Because, as will be shown later, the gross structural weights of conventional and OHS aircraft for comparable missions are essentially similar, Table 1 was assumed to be

Table 1 Component weight distribution

Component name	Subtotals, %	Weight, %
Engines (including propellers, etc.)	——	12
Fuselage (including landing gear)	——	18
Main plane plus stabilizers, etc.[a] (30% of total): breakdown: tail, etc. 0.3 $(S_{TH}/S_w)_{OHS}$ % wing: 30% - tails, etc. %	60	30
Fuel	——	15
Payload	40	25
——	$\Sigma = 100$	$\Sigma = 100$

[a]Allows for wing weight increasing with aspect ratio for OHS configurations (see Fig. 2). This wing weight also assumed to apply to conventional configurations.

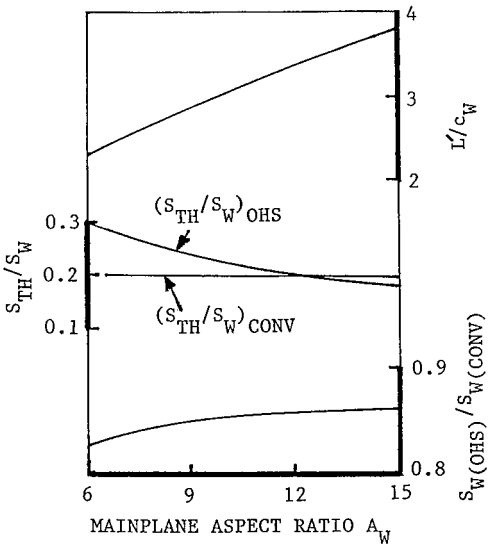

Fig. 2 OHS geometry, as a function of wing aspect ratio A_w compared with the geometry of comparable conventional aircraft.

applicable to both aircraft types. To simplify, slightly, the design exercise, the decision was made to evaluate the location of the center of pressure of the NACA 2412 section explicitly to establish the chordwise location of the lift and thereby eliminate the need to take into account separately the airfoil pitching moment, by means of the standard relationship:

$$x_{cp}/c_w = x_{ac}/c_w - C_{m(ac)}/C_{LW} \tag{1}$$

where, for an NACA 2412 section, $x_{ac}/c_w = 0.25$ and $C_{m(ac)} = -0.05$.

Because the main-plane and stabilizer surfaces selected were identical to those employed in a comparison of the aerodynamic performances of OHS and comparable conventional aircraft,[4] data from that study were employed to generate geometric information required for the design exercise. This information is displayed in Fig. 2, which presents, vs wing aspect ratio A_w, the ratio of horizontal stabilizer planform area to wing area (S_{TH}/S_W) for both the OHS and comparable conventional aircraft. Figure 2 also presents the wing, or main plane, area ratio $S_{w(OHS)}/S_{w(CONV)}$ and the effective dimensionless tail-arm length, L'/c_w for the OHS vehicles. The ratio $S_{w(OHS)}/S_{w(CONV)}$ is for all practical purposes independent of C_{LW} and, as implied in Fig. 2, can be regarded as conforming to a unique relationship over the range $0.4 \le C_{LW} \le 1.0$. On the basis of an earlier aerodynamic study,[4] the pitch static margins of the OHS and corresponding conventional configurations represented in Fig. 2 were 0.23 with the center of gravity located at $0.65c_w$ and $0.25c_w$ for the OHS and conventional configurations, respectively. The static margin is defined as the distance from the center of gravity to the neutral point divided by the mainplane chord c_w.

Wing-Root Bending Moments

Figure 3 is a force diagram showing, in a simplified manner, forces contributing to the wing-root bending moments for an OHS configuration. It was assumed for the design exercise that all the fuel for the OHS configurations is carried in the wing, but, because the vehicle center-of-gravity design point occurs at, or close to, 65% of the main-plane chord c_w, aft of the wing leading edge the fuel load is contained in narrow tanks extending over the full span of the wing. For comparative conventional designs wider fuel tanks are feasible because the center of gravity of these vehicles is closer to the quarter-chord station. An inherent possibility for OHS configurations is to employ the tail-support booms as wing-tip tankage. This provides a bending moment relief to the wing, but advantage of this possibility was not incorporated into the design exercise because, without the specific provision of wing-tip tanks, a corresponding option was not available for the simple conventional configurations used in the comparative study. The conventional configurations would, presumably, employ a nose-mounted twin-pack engine instead of the centerline twin-engined arrangement of the candidate OHS aircraft shown in Fig. 1.

An indication of the approximate fuel-carrying potential of the tail-support booms of OHS aircraft is presented in Fig. 4 based on the assumption that the center of gravity of the fuel load should correspond to the vehicle design-point center of gravity at 65% of the main-plane chord aft of the wing leading edge. It can be seen, from Fig. 4, that the fuel-carrying potential of the tail-support booms diminishes as A_w is increased. The boom diameter was, for each case, taken to be 1.5 times the 12% c_w wing maximum thickness. An alternative use for the space within the booms is to house retractable outrigger undercarriage equipment for OHS aircraft provided with bicycle main gear mounted in the main fuselage.

Wing-root bending moments (BM) of OHS aircraft at different load conditions as ratios of corresponding BMs of corresponding conventional configurations (CONV) of equal gross weight are presented, as functions of main-plane aspect ratio A_w, in Fig. 5 for a wing lift coefficient of 0.6 a value close to the optimum for OHS configurations.[4] The labels A, B, and C assigned to the curves of Fig. 5, and subsequent diagrams, refer to the empty dry, full payload

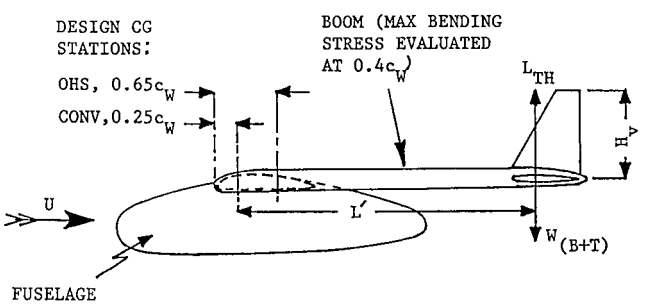

Side elevation

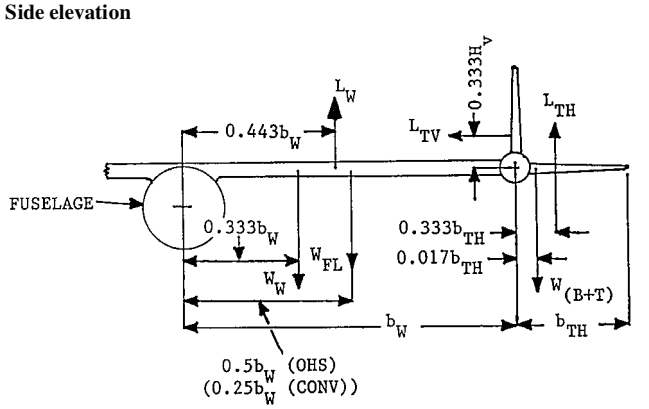

View looking downwind

Fig. 3 Load application diagram for loads giving rise to wing-root bending moments in OHS aircraft. Weights and lift refer to half total values for aircraft.

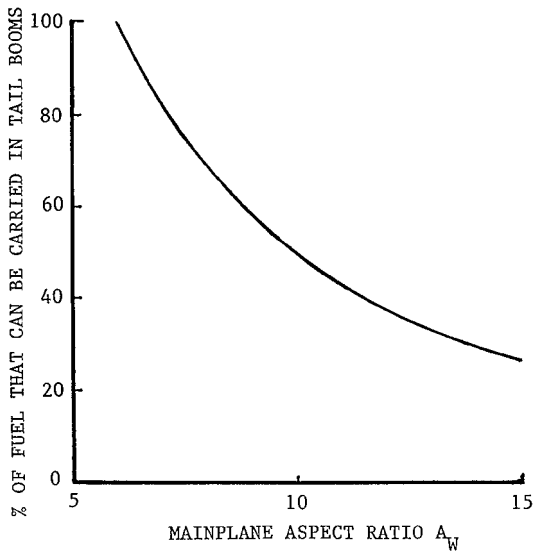

Fig. 4 Potential fuel tankage capacity in the tail booms of OHS aircraft.

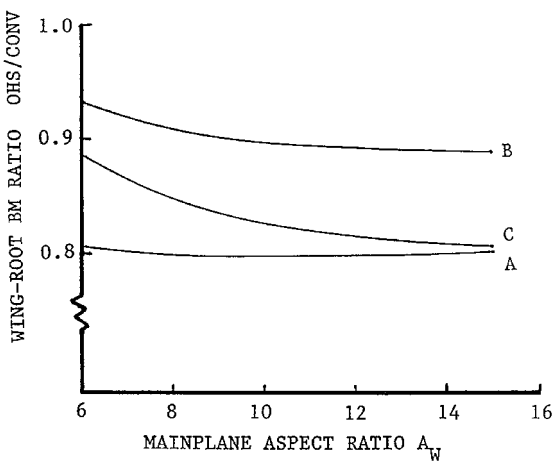

Fig. 5 Wing-root bending moment loads vs A_w for OHS aircraft as a fraction of corresponding loads in conventional aircraft $C_{LW} \equiv 0.6$.

no fuel, and full payload plus maximum fuel loading conditions, respectively. The results shown in Fig. 5 may, at first glance, seem surprising. However, the main planes of the conventional vehicles are larger in planform area, approximately 18% larger, than those of the corresponding OHS aircraft as a result of a small negative tail-lift force and also the additional lift needed to compensate for the positive lift of the OHS horizontal stabilizers. Counter to this, for the OHS case wing-root BM contributions are derived from both the horizontal and vertical tail surfaces although the weight of the tail structure helps to offset these. The relative aerodynamic loads were derived from the analysis for prior work.[4] Figure 6 presents the wing-root BMs of OHS aircraft relative to the maximum values for corresponding conventional configurations also for a main-plane lift coefficient C_{LW} of 0.6 yielding, as might be expected, generally lower values than those of Fig. 5. Figure 7 shows wing-root BM ratios for an aspect ratio A_w of nine vs mainplane lift coefficient C_{LW}. It is apparent from Fig. 7 that the wing-root BM ratio increases as C_{LW} increases.

Wing-Root Torsional Loads

Forces contributing to wing-root torsional loading are identified in Fig. 8 together with the loads contributing to tail-support boom torsional and bending loads. The relative load values were obtained as a byproduct of an earlier analysis.[4] The distance x_{cp} from the main-plane leading edge to the effective location of wing lift was

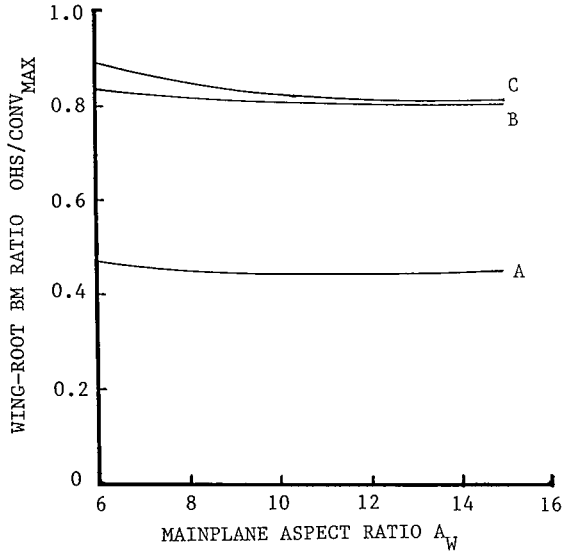

Fig. 6 Wing-root bending moment loads vs A_w for OHS aircraft as a fraction of the corresponding maximum loads, as a function of aspect ratio, for conventional aircraft $C_{LW} \equiv 0.6$.

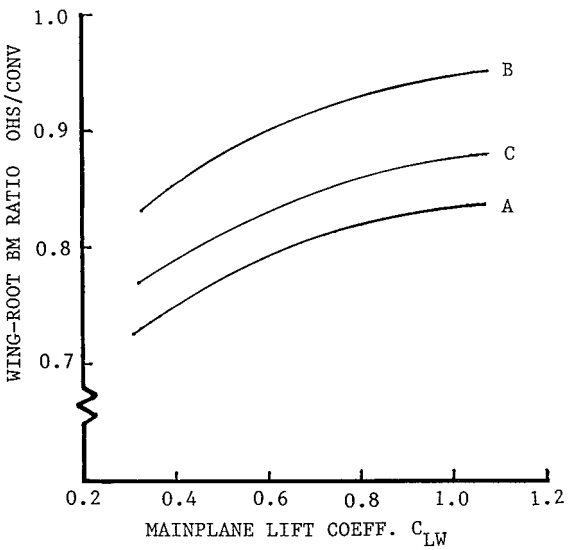

Fig. 7 Wing-root bending moment loads for OHS aircraft, as a function of C_{LW}, divided by the corresponding loads for conventional configurations $A_w = 9$.

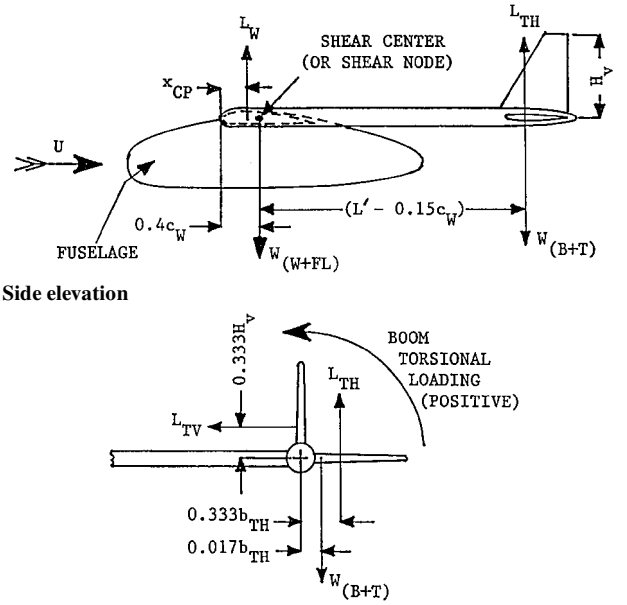

Fig. 8 Load application diagram for torsional loading of OHS aircraft. Weights and lifts refer to half of the total values for aircraft.

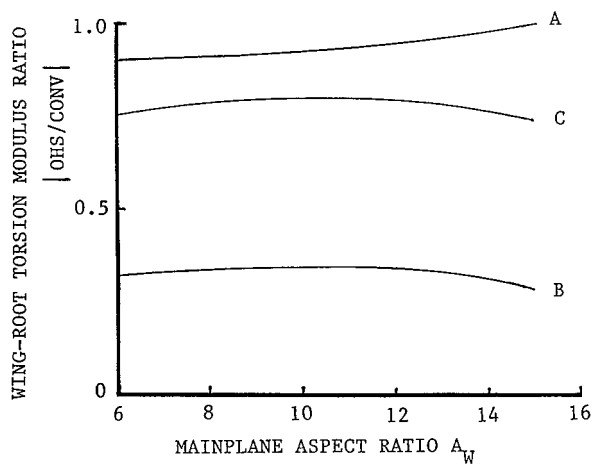

Fig. 9 Ratio of wing-root torsional load modulus vs A_w of OHS aircraft based on the corresponding torsional loads in conventional aircraft $C_{LW} \equiv 0.6$.

obtained from Eq. (1). The location of the shear center, or shear node, was assumed to lie at 40% of the wing chord c_w aft of the wing leading edge. The airfoil section selected for the main plane was an NACA 2412 and that for the tail surfaces was a NACA 0012 (Ref. 5).

The modulus (i.e., value independent of sign) of the OHS wing-root torsional load as a fraction of that for corresponding conventional configurations is presented in Fig. 9 vs aspect ratio A_w. A modular ratio was employed to compensate for sign reversals, thereby making the diagrams more compact. Figure 10 displays the same ratio, for $A_w = 9$, vs the mainplane lift coefficient C_{LW}. The relatively high ordinate values, nearly 2.4 at $C_{LW} = 0.4$, do not reflect high OHS loadings in the absolute sense as can be seen from Fig. 11, which is a replot of Fig. 10 referenced not to the local value of the torsional load but to the maximum torsional load occurring in the conventional configuration, which occurred when $C_{LW} = 1.0$ with full fuel and payload condition (i.e., load condition C). The ordinate value of the horizontal line representing loading case A is positive: the ordinate values of the other two lines are negative, for each case, in Figs. 9–11; the vehicle center of gravity was set, as for the bending moment cases, at 65% of c_w aft of the wing leading edge.

Wing-Tip Torsional Loads

For conventional aircraft no torsional loads are transmitted through wing tips into the wing structure. Hence the OHS situation in which torsional loads are transmitted into the wing tips from the tail-support booms does not have a parallel in conventional configurations. A comparison was therefore made between the wing-tip torsional load inputs as a ratio of the greatest wing-root torsional load associated with a conventional configuration namely that prevailing when $C_{LW} = 1.0$ under a fully fueled maximum payload operating mode. The result of this study is presented in Fig. 12. The negative ratios imply a nose-down torque applied to the wing tips. The positive, nose-up torque is caused by the tail lift being, for such conditions, less than the weight of the booms and tails. The maximum torque ratio of nearly 1.4 shown in Fig. 12 is not as alarming as it might seem at first glance. This point is well illustrated by means of a simple design study based on the OHS commuter type aircraft depicted in Fig. 1 with the weight distribution data presented in Table 1.

An 18-passenger (or so) commuter aircraft of the type shown in Fig. 1 is of 66.7 kN (15,000 lbf) gross weight, 19.2-m (63-ft) wing span and 2.13-m (7-ft) uniform chord (i.e., $A_w = 9$). It can be

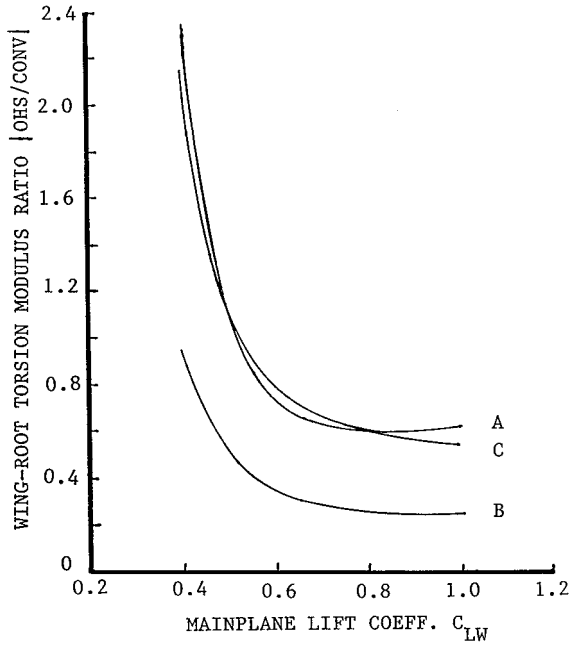

Fig. 10 Variation of wing-root torsional load modulus vs C_{LW} for OHS aircraft based on the corresponding torsional loads in conventional aircraft $A_w = 9$.

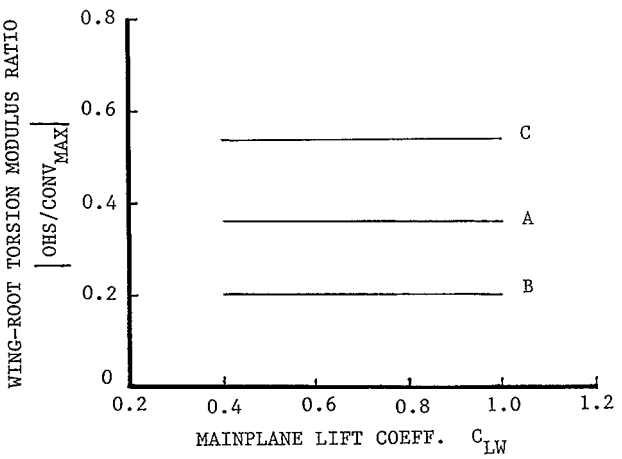

Fig. 11 OHS wing-root torsional load modulus vs C_{LW} based on the maximum torsional load; when $C_{LW} \equiv 1.0$, in conventional aircraft $A_w = 9$.

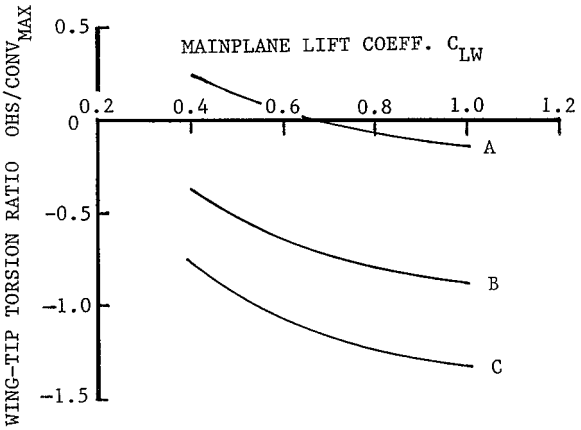

Fig. 12 OHS wing-tip torsional load vs C_{LW} divided by the maximum wing-root torsional load; when $C_{LW} \equiv 1.0$, in conventional aircraft $A_w = 9$.

shown that when $C_{LW} = 1.0$ and a simple tubular main spar provides all of the strength of the wing and the diameter of the main spar nearly equals the wing maximum thickness of 12% of the chord resulting in a spar outer diameter of 254 mm (10 in.) then with a wall thickness of 15 mm (0.59 in.) the maximum bending-induced direct stress at the wing root is 140.9 MN/m^2 (10.22 T/in^2), a value consistent with a good fatigue resistance (5×10^8 cycles) quoted in the literature for 7075-T6 grade aluminum.[6,7] This primitive, tubular, main spar is well within the permitted weight limit of the wing with an allowance for the remainder of the wing structure. The corresponding maximum shear-stress level in the tubular main spar is 8.27 MN/m^2 (0.6 T/in^2) at the tips with an average value in the main spar of 5.79 MN/m^2 (0.42 T/in^2) or approximately only 4% of the wing-root direct stress level. This translates, assuming no stiffening of the main spar as a result of the remaining wing structure, into a twist of the main spar of less than 1 deg at the tips. These results suggest, within the limitations imposed by the simplistic design approach, that wing torsional loading does not seem to be a major weight-driving problem.

A study of the OHS tail-support booms indicates that with a tubular aluminum boom of a diameter equal to 1.5 times the maximum wing thickness a boom wall thickness of 3.2 mm (0.126 in.) results in a maximum shear stress of 10.34 MN/m^2 (0.75 T/in^2) with a maximum direct stress, caused by bending, of 62 MN/m^2 (4.5 T/in^2). The maximum boom torsional deflection, or twist, is 0.65 deg. Simple tubular tail-support booms of the type developed are also acceptable from the viewpoint of their weight.

An attempt to follow up on the OHS wing design exercise with the design of a corresponding structurally and geometrically similar wing for a comparable conventional aircraft resulted in a heavier wing than that of the OHS vehicle. However, the conventional aircraft would, most likely, employ a tapered wing resulting, relative to an OHS wing of constant or nearly constant chord, in a significant weight saving. The weight saving could be at least 10% with a taper ratio of 0.5. It appears, therefore, that when the weight of the OHS tail booms is equated to that of the aft fuselage of a comparable conventional aircraft, and with essentially equal tail surface weights in both cases, that at least to a first approximation OHS and comparable conventional aircraft are likely to be of equal structural weight.

Variation of Center-of-Gravity Location

The effective permitted fore-and-aft range of variation of the location of the c.g. of OHS aircraft expressed as a fraction of wing chord c_w is $0.5 \leq$ c.g. ≤ 0.75. The lower limit is caused, essentially, by the diminished tail lift resulting from forward movement of the c.g. location from an optimum station in the region of $0.60 \rightarrow 0.65c_w$. The aft location of $0.75c_w$ is dictated by the requirement for static stability in pitch that the c.g. must be located ahead of the neutral point. The neutral point location occurs, typically for OHS configurations, at about $0.8c_w$, a value that should, of course, be verified for each design.

Movement of the c.g. location has a more dramatic influence on the wing-root torsional load than wing-root bending loads. The wing-root torsional load, presented as a modulus to accommodate negative as well as positive torsional loads, is plotted as a fraction of the maximum torsional load, when $C_{LW} = 1.0$, attained with a comparable conventional configuration when fully loaded and fueled. The resultant wing-root torsional modulus is plotted vs the c.g. location, as a fraction of c_w aft of the wing leading edge, in Fig. 13. The V-shaped curves are a consequence of the torsional load changing from positive, via zero, to negative from the left to the right side of the figure. The corresponding wing-root bending moment ratio is presented vs c.g. location in Fig. 14. The maximum value of the conventional-configuration bending-moment occurs when $C_{LW} = 0.4$ for the fully loaded and fueled condition. As can be seen from Fig. 14, the wing-root bending moment increases from the left- to the right-hand side of the figure, the opposite gradient to that caused by torsional loadings presented in Fig. 13.

The feasible range of variation of the c.g. location as a fraction of the main-plane chord aft of the wing leading edge, namely,

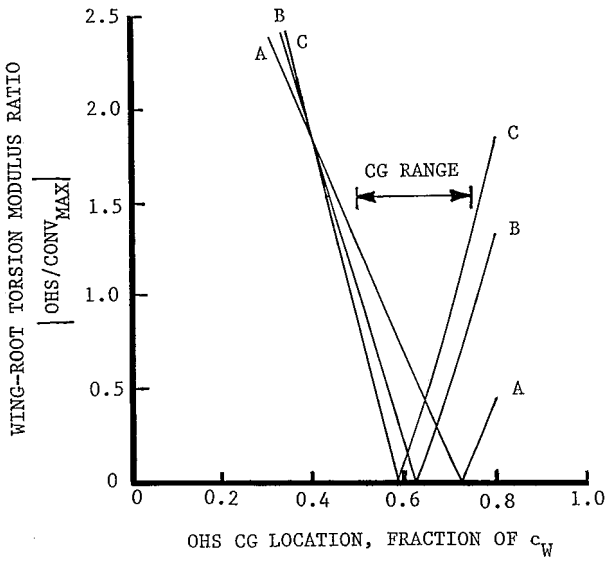

Fig. 13 OHS wing-root torsional load modulus vs c.g. location, based on the maximum torsional load; when $C_{LW} \equiv 1.0$, in conventional aircraft $A_w = 9$, and $C_{LW} \equiv 0.6$.

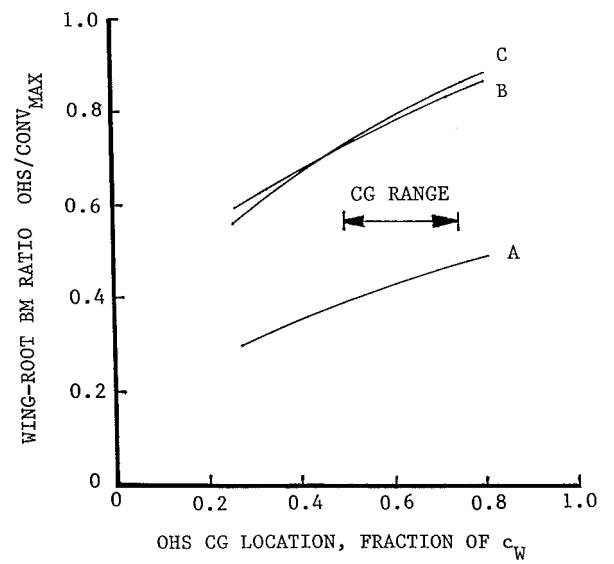

Fig. 14 OHS wing-root bending moment load vs c.g. location based on the maximum bending moment load; when $C_{LW} \equiv 0.4$, in conventional aircraft $A_w = 9$, and $C_{LW} \equiv 0.6$.

$0.5c_w \leq$ c.g. $\leq 75c_w$ corresponds, for the aircraft of Fig. 1, to a movement of the payload c.g. from a forward location close to the bulkhead separating the cockpit from the passenger space to an aft location close to the rear of the passenger space.

Flutter Susceptibility

Consideration of the practical feasibility of OHS configurations demands that attention be paid to flutter characteristics. Flutter of the inbound portions of the wings of conventional, single fuselage aircraft is essentially unknown because of the presence of the horizontal stabilizer frustrating and dampening such motion although in at least two, possibly more, cases flutter of an insufficiently rigid horizontal stabilizer has been a problem. In much the same manner the horizontal stabilizer surfaces of OHS configurations can flutter, much as is the case for conventional aircraft, if they are insufficiently stiff. Additionally the vertical stabilizer surfaces also have the potential to flutter in the manner of the horizontal tail surfaces. Flutter of the vertical surface, or surfaces, of conventional aircraft can also occur but is probably less likely than with OHS aircraft because of the (lateral) lift-like, inwardly directed, forces associated with the OHS vertical tail surfaces.

Relative to a conventional configuration, each tail boom and attached tail surfaces of an OHS configuration are analogous to the rear fuselage, with attached tail surfaces, of a conventional aircraft. Hence the outer portions of the mainplane of an OHS configuration are much less likely, in general, to develop flutter than those of a conventional design because of the presence of tail surfaces attached to the wing tips by means of the tail-support booms. This consideration is a consequence of the tail surfaces conspiring to prevent flutter and thereby suppress any flutter tendency of the outboard portions of the main plane. If wing flutter were to develop, it would cause the attached horizontal stabilizers to flap upward and downward in pitch as a result of wing torsional motion and in torsion as a result of wing bending. Such oscillatory motions are described, in general terms, by second-order differential equations of the form of Eq. (2):

$$M\ddot{\theta} + F\dot{\theta} + K\theta = 0 \tag{2}$$

When θ is the linear displacement of the tail structure from the origin of the oscillation, M is the effective mass of the tail; F represents, when positive, the active damping force per unit of tail oscillating velocity, and K is the elastic stiffness of the structure. Alternatively when θ represents the angular displacement of the tail and M is replaced by I, the moment of inertia of the tail and F and K are correspondingly expressed in angular format; Eq. (2) has a similar meaning with F, when positive, representing a damping torque per unit of tail angular velocity.

For both the linear and angular tail motions described, F serves to damp tail oscillations and hence damp flutter of the outer portions of the mainplane. The mechanism by which this occurs is illustrated, for a linear case, in Fig. 15. Figure 15a applies to a simple flapping motion, Fig. 15b to a combined flapping and pitching motion. In both cases F acts to oppose the tail oscillating motion. It can also be shown that it does the same for torsional oscillation of the tail as a result of wing flapping and/or torsional elastic twisting of the tail boom.

Because the fuselage constitutes a large mass at the wing center, it appears that the only other likely wing flutter mode has an antinode located on each half of the main plane at a station between the fuselage and the wing tip. However this, it seems, is less likely to be a troublesome region than the outboard portions of the mainplanes of conventional aircraft.

A flutter analysis of a full-scale, high-aspect-ratio, high-altitude OHS-type, environmental monitoring uninhabited air vehicle of 31.4-m (103-ft) span was carried out by Scaled Composites, Inc. It was found that flutter, for that particular aircraft, was not a concern within the mission envelope.

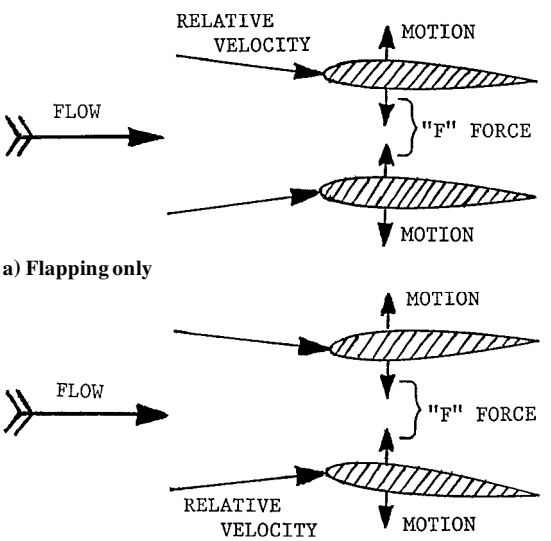

Fig. 15 Generation of aerodynamic damping force F.

Additional Considerations

Several additional factors should be taken into account relating to the practicality of OHS aircraft:

1) OHS aircraft of anything but the smallest type appear to be excellent candidates for the application of fly-by-wire technology as a result of the relative complexity of connecting the elevator and rudder controls to the cockpit by purely mechanical means. Because fly-by-wire systems are already in use, this does not, therefore, define a need for the development of new control technology.

2) To minimize the risk of ground strikes during takeoff and landing, it is desirable to employ high-wing configurations for OHS aircraft. An alternative is to employ a low-wing configuration with a relatively tall undercarriage to establish an adequate ground clearance.

3) It is generally more difficult to attach the main undercarriage to the wing of a nonswept, straight-winged, OHS configuration caused by the vehicle c.g. location lying substantially aft of that of a conventional aircraft. Hence a wing-supported main gear imposes a considerable torsional loading on the wing. A solution is to employ a fuselage-attached main gear, possibly housed in "blisters," as is the case for a number of conventional high-winged aircraft, or alternatively, to use a bicycle-type undercarriage in conjunction with outrigger stabilizers.

4) A high subsonic Mach-number OHS jet (turbofan) aircraft should, ideally, differ from the second World War era work of Blohm und Voss, referred to earlier, featuring aft-swept wings and, instead, employ wings that, relative to the fuselage, are swept forward. Relative to the horizontal stabilizer surfaces, such a wing arrangement is swept-aft as in most conventional swept-wing vehicles. This arrangement represents a structurally stable OHS configuration. It also has the additional advantage of providing the possibility of fuel tankage in the wing closer to the vehicle c.g. than is feasible with a straight-winged design such as that of Fig. 1. Furthermore, the forward-swept wing makes it possible to mount the main undercarriage on the wing, fairly close to the main spar, while avoiding wing torsional-loading problems. Additionally the concept of the independence principle[8] should allow the potential benefits of forward sweep to be realized with an OHS configuration without encountering the structural difficulties that would otherwise be incurred when forward sweep is applied to an otherwise conventional aircraft.

In view of the prediction[9] that turboprop commuter aircraft are losing favor with the traveling public despite more efficient fuel usage relative to jet aircraft, it may well be that the suggestion of a forward-swept-wing OHS configuration is appropriate.

Conclusions

The comparative study of the relative aerodynamically and gravitationally generated critical loads, and stresses, in light transport aircraft of the OHS and conventional types led to the following conclusions:

1) The potential for fuel storage in the tail booms of OHS aircraft diminishes, for booms restricted to a diameter equal to 150% of the maximum mainplane thickness, as the mainplane aspect ratio A_w increases. At an A_w value of 14, the boom fuel capacity is only 30% of that when $A_w = 6$.

2) Ignoring the potential for obtaining, for OHS aircraft, wing bending moment relief by carrying fuel in the tail-support booms, it was found that, generally, the wing-root bending moment loads for the OHS version of the aircraft were, for equal wing lift coefficients, wing aspect ratios and vehicle gross weights less than those of a corresponding conventional configuration. This was a result of a combination of the planform area of the wing of the OHS vehicle being, due to the lifting tail surfaces, typically 15% smaller than the wing of the conventional aircraft and also due to bending moment relief from the weight of the booms and tail surfaces attached to the wing tips. These influences more than countered the additional bending moments acting on the OHS wing because of the lift of the horizontal tail surface and the aerodynamic loading acting on the vertical tail.

3) The torsional loading at the wing root of the OHS aircraft was generally less than the corresponding loading of a comparable conventional vehicle. This was a result of the negative (nose-down) moment applied at the wing-tip countering the positive pitching moment resulting from wing lift. This situation changed dramatically for very low wing lift coefficient values C_{LW}, a condition under which the tail lift coefficient, normally about half the wing lift coefficient, was insufficient to generate a lift equal to the weight of the tail structure. Wing-tip torsional loads, under realistic flight conditions, exceeded the wing-root values of comparable conventional aircraft. However the resultant stress levels were low enough to not constitute a stress problem.

4) Movement of the vehicle c.g. location significantly from the optimum location at 60–65% of the wing chord aft of the wing leading edge had a fairly strong influence on wing-root shear loads and a relatively small influence on corresponding bending moment loads. Within the c.g. range $0.55c_w \leq \text{c.g.} \leq 0.72c_w$, there were no problems caused by excessive loads.

5) It was concluded that the presence of outboard horizontal stabilizers inhibits the likelihood of flutter occurring in the outboard wing areas of OHS aircraft. Flutter can occur, as for conventional aircraft, in the tail surfaces of OHS vehicles.

Acknowledgments

The writer acknowledges the help of numerous undergraduate students of the Department of Mechanical and Manufacturing Engineering of the University of Calgary who have, over a period of eight years, contributed to the building of flying, radio-controlled, powered models of OHS aircraft. The assistance of members of the model aircraft community who have served as pilots for these models is also acknowledged.

References

[1] Kentfield, J. A. C., "Aircraft Configurations with Outboard Horizontal Stabilizers," Dept. of Mechanical Engineering, Univ. of Calgary, Rept. 440, Calgary, Alberta, Canada, Jan. 1990.

[2] Kentfield, J. A. C., "Case for Aircraft with Outboard Horizontal Stabilizers," *Journal of Aircraft*, Vol. 32, No. 2, 1995, pp. 398–403; also AIAA Paper 94-0498, Jan. 1994.

[3] Kentfield, J. A. C., "The Aspect-Ratio Equivalence of Conventional Aircraft with Configurations Featuring Outboard Horizontal Stabilizers," *Society of Automotive Engineers Journal of Aerospace, Sec. 1*, Vol. 106, Oct. 1997, pp. 1733–1741; also Society of Automotive Engineers Paper 975591, Oct. 1997.

[4] Kentfield, J. A. C., "Influence of Aspect Ratio on the Performance of Outboard-Horizontal-Stabilizer Aircraft," *Journal of Aircraft*, Vol. 37, No. 1, 2000, pp. 62–67; also AIAA Paper 99-0531, Jan. 1999.

[5] Abbott, I. H., and von Doenhoff, A. E., *Theory of Wing Sections*, Dover, New York, 1959, pp. 462–479.

[6] Faires, V. M., *Design of Machine Elements*, 4th ed., Macmillan, New York, 1965, pp. 63, 64, and 566.

[7] Spotts, M. F., *Design of Machine Elements*, 5th ed., Prentice–Hall, Upper Saddle River, NJ, 1978, pp. 661–665.

[8] Jones, R. T., *Wing Theory*, Princeton Univ. Press, Princeton, NJ, 1989, pp. 91–98.

[9] Butterworth-Hayes, P., "Turboprop Airliners Face a Grim Future," *Aerospace America*, Vol. 36, No. 8, 1998, pp. 4–6.